OPEN ACCESS
Journal of Multidisciplinary Applied Natural Science Vol. xx No. xx (xxxx) https://doi.org/10.47352/jmans.2774-3047.352
Check for updates
Research Article

Synthesis of Chitosan-based Materials with Ester-benzoate Modification and Its Application as An Antimicrobial Agent

Devi Ratnawati*, Risky Hadi Wibowo, Vicka Andini, Evi Maryanti, and Yehezkiel Steven Kurniawan

Received : October 9, 2025	Revised : December 17, 2025	Accepted : December 29, 2025	Online : January 22, 2026

Abstract
Microbial infections pose serious threats to human health, emphasizing the need to develop effective antimicrobial materials. This study aims to synthesize, characterize, and evaluate the antimicrobial properties of ester vanillin-benzoate (**1**) and its chitosan-based composite material (**2**). Furthermore, the synthesized compound was tested for antibacterial and antifungal activities against *Staphylococcus aureus*, *Bacillus subtilis, Escherichia coli, Pseudomonas aeruginosa*, and *Candida albicans* using the Kirby-Bauer diffusion method. The synthesized compounds were effective against *S. aureus* and *B. subtilis* but had minimal action against *P. aeruginosa*, *E. coli*, and *C. albicans*. The formation of the Schiff-base composite could increase its antibacterial activity, indicating a synergistic effect arising from the combination of compound **1** and chitosan.

Keywords: antibacterial, chitosan, composite material, ester vanillin benzoate, Schiff base reaction

1. INTRODUCTION

Chitosan is a biopolymer derived through the deacetylation of chitin (β-(1→4)-2-amino-2-deoxy-D-glucopyranose) [1][2]. It is widely recognized for its remarkable chelating ability, which emerges from the amount of primary amino groups dispersed uniformly along its molecular chains [3]. Chitosan is the second most abundant natural polysaccharide after cellulose. It is well-known for its remarkable biocompatibility, biodegradability, and non-toxicity, making it highly valuable for a wide range of applications [4][5]. Although chitosan is insoluble in water, it rapidly dissolves in aqueous solutions of organic acids, including acetic, formic, and citric acids, as well as diluted hydrochloric acid, resulting in viscous solutions [6]. Chitosan has drawn significant interest in research due to its cationic nature, biocompatibility, biodegradability, non-toxicity, and diverse biological activities [7]-[9]. Chemical alteration, particularly focusing on its hydroxyl and amino functional groups, can increase its physicochemical properties [10].

Schiff bases are a class of organic compounds characterized by the presence of an imine (azomethine) group (H–C=N). These compounds are typically formed when amino groups readily react with aldehydes or ketones [11]. When chitosan interacts with aldehydes or ketones, it forms aldimines or ketoimines, respectively, through a condensation process that releases a water molecule [12]-[14]. Functionalized chitosan with Schiff base derivatives are typically synthesized by condensation of chitosan's amino groups with the carbonyl groups of aldehydes or ketones, generating stable imine linkages [15]-[17]. Under neutral conditions, chitosan rapidly reacts with both aromatic and aliphatic aldehydes or ketones to produce Schiff bases [18][19]. The efficiency of this synthesis can be improved by employing different solvents, such as acetic acid, ethanol, methanol, or their mixtures [20]-[22]. In addition, chitosan Schiff bases have been synthesized using a number of solvents, including dimethylformamide (DMF), water, and ionic liquids [23][24]. Among the various chitosan alterations, the formation of Schiff base derivatives is one of the most important [25][26]. The introduction of imine groups significantly enhances chitosan's biological potential, improving its anti-inflammatory, antioxidant, anticancer, antibacterial, and antifungal properties [27]-[30].

Previous studies on the antimicrobial activity of chitosan and its derivatives, particularly chitosan Schiff bases, have highlighted their significant potential as antibacterial agents [31][32]. A

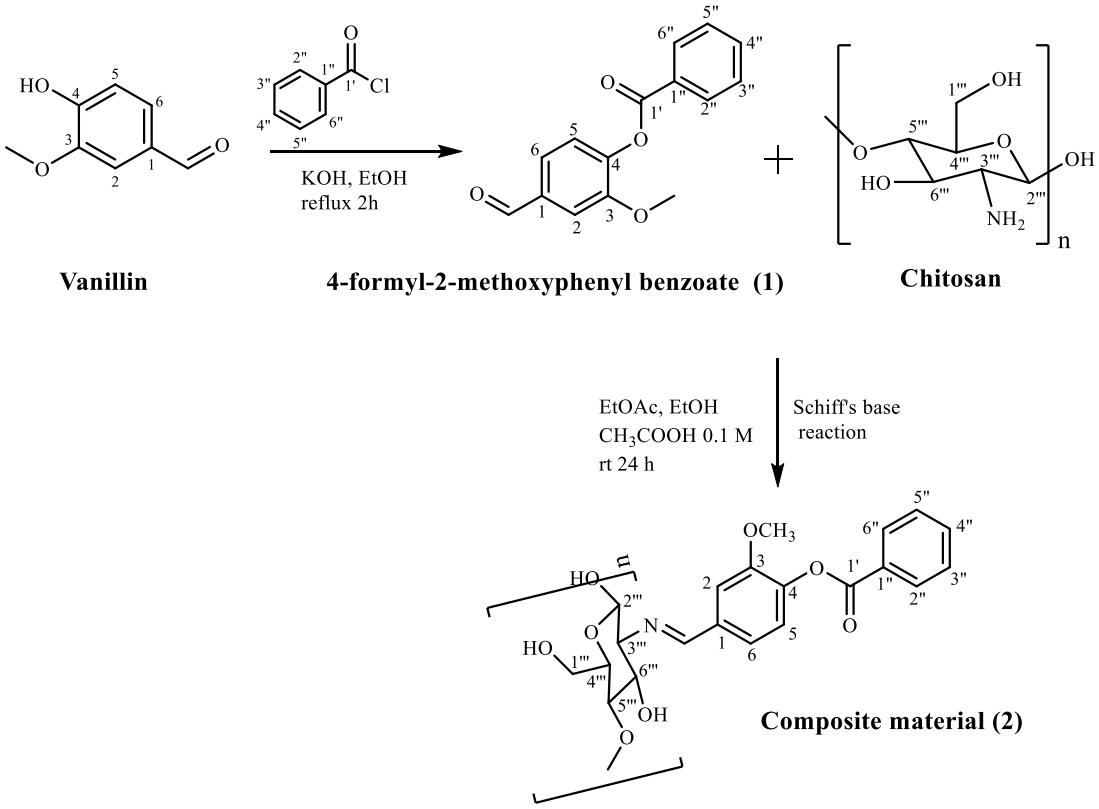

Figure 1. Synthesis of composite material (**2**).

growing number of research has demonstrated that chitosan derivatives, particularly those modified into Schiff bases, exhibit increased antibacterial and antifungal activity against a range of pathogenic microorganisms [33][34]. Schiff bases, which are generated by functionalized chitosan containing aromatic ester groups, have been demonstrated to possess potent antibacterial properties against several common pathogens, including *Staphylococcus aureus*, *Escherichia coli*, and *Candida albicans* [35][36]. To our knowledge, there has been no publication on the antibacterial activity of Schiff bases derived from chitosan and vanillin-benzoate. In this work, vanillin was esterified using benzoyl chloride to produce vanillin benzoate ester, which was then combined with chitosan through a Schiff base reaction to form a composite material. This is notable because such a substance might increase the economic value of vanillin, one of Indonesia's plentiful and valuable natural products.

This study explores the synthesis and antimicrobial properties of ester vanillin-benzoate (**1**) and its composite material (**2**), building on prior research on chitosan and Schiff base derivatives. The structural features of both compounds were thoroughly characterized using multiple spectroscopic techniques, including Fourier transform infrared spectroscopy (FTIR), nuclear magnetic resonance (NMR) spectroscopy, gas chromatography–mass spectrometry (GC–MS), X-ray diffraction (XRD), and Raman spectroscopy. In addition, the surface morphology of the samples was examined using scanning electron microscopy with energy-dispersive X-ray spectroscopy (SEM-EDX). These extensive characterization procedures provided valuable insights into the structural and morphological characteristics of the synthesized chitosan derivatives, highlighting their potential as antibacterial agents.

2. MATERIALS AND METHODS

2.1. Materials

The study employed analytical-grade chemicals (Merck), including vanillin ($C_8H_8O_3$), potassium hydroxide (KOH), ethanol (CH_3CH_2OH), ethyl acetate ($CH_3CO_2C_2H_5$), benzoyl chloride (C_6H_5COCl), and acetic acid (CH_3COOH), as well as culture media such as tryptic soy agar and

Sabouraud dextrose agar.

2.2. Methods

2.2.1. Synthesis of 4-formyl-2-methoxyphenyl benzoate (*1*)

A mixture of KOH (0.56 g, 10 mmol) in 10 mL of 96% ethanol, benzoyl chloride (1.70 mL, 10 mmol), and vanillin (1.52 g, 10 mmol) was refluxed for 2 h. The progress of the reaction was monitored using thin-layer chromatography (TLC) with an ethyl acetate:*n*-hexane solvent system (3:2 v/v). Next, 2 mL of a 5% w/v KOH solution and 30 mL of distilled water were slowly added to the mixture, which was then stirred for another 30 min before being poured into an ice bath. The target product was obtained by filtering the resulting solid, then drying and recrystallizing it in ethanol (see Figure 1).

2.2.2. Synthesis of Composite Material (*2*)

One mmol of chitosan (161.97 mg, DD 97.69%) was combined with 30 mL of 0.1 M CH_3COOH overnight at room temperature. Subsequently, one mmol (282.30 mg) of 4-formyl-2-methoxyphenyl benzoate (**1**) was dissolved in 10 mL of ethyl acetate and added to the chitosan solution, followed by 10 mL of ethanol. The same procedure was applied to dissolve chitosan for the reaction. After 24 h, the precipitate was filtered, dried, and its melting point was determined (see Figure 1).

2.2.3. In Vitro Antimicrobial Assays

The Kirby–Bauer disc diffusion method was used to assess antibacterial activity. Utilizing these methods, the antibacterial properties of chitosan and its derivatives were evaluated against *Candida albicans* (ATCC 90028), two Gram-positive bacteria (*Staphylococcus aureus*, ATCC 25923 and *Bacillus subtilis*, ATCC 6633), and two Gram-negative bacteria (*Escherichia coli*, ATCC 8739 and *Pseudomonas aeruginosa*, ATCC 9027). The antimicrobial activity assay used 10 mg of the sample dissolved in 100 µL of ethyl acetate in a microtube and was thoroughly vortexed. Subsequently, 1 mL of the test microbial culture was added to an Erlenmeyer flask containing 100 mL of tryptic soy agar (TSA) for bacterial tests or Sabouraudd dextrose agar (SDA) for fungal tests. To assess antimicrobial activity, sterile paper discs (Whatman No. 42, 6 mm in diameter) were dipped in 10 µL of the sample solution and placed at the center of the medium containing the test microbes. The media were incubated for 24 h at 37 °C for

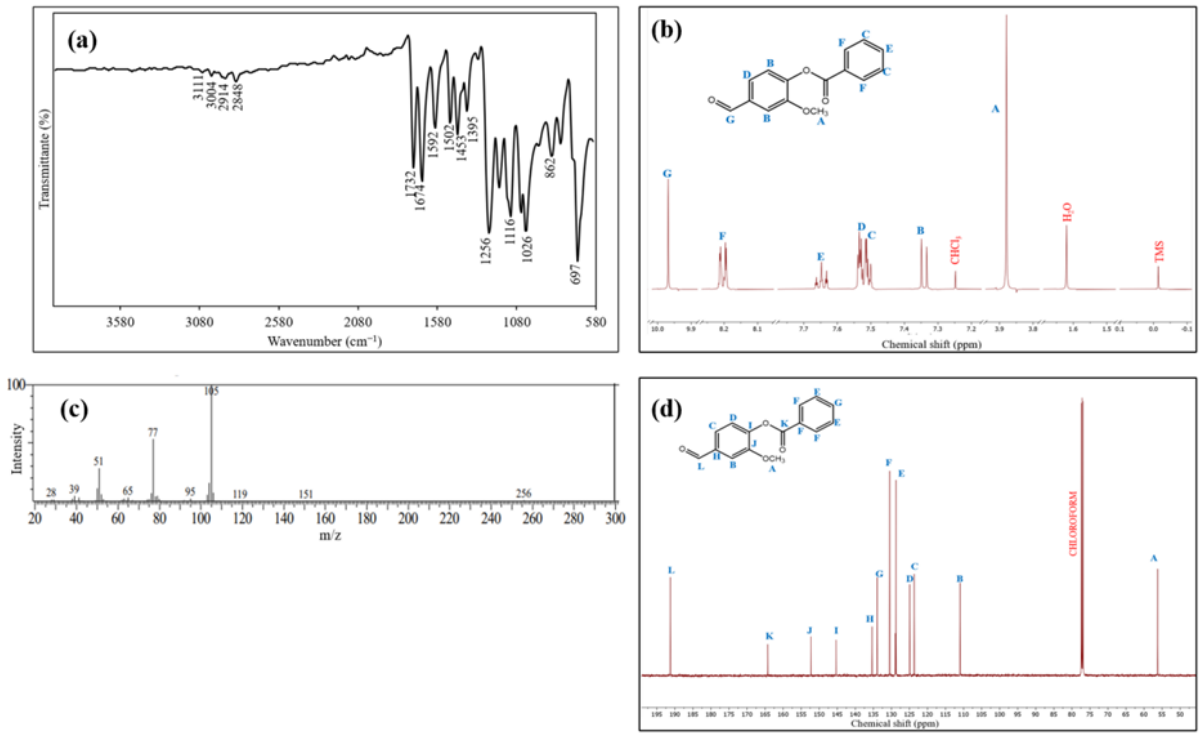

Figure 2. (a) FTIR, (b) 1H–NMR, (c) MS, and (d) 13C–NMR spectrum of ester vanillin-benzoate (1).

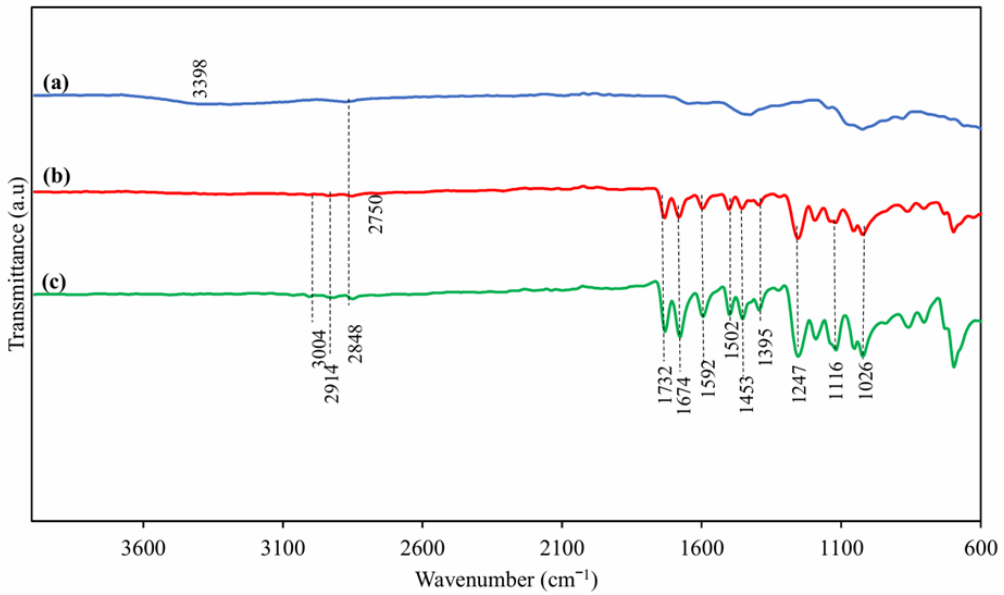

Figure 3. FTIR spectra of (a) chitosan (blue line), (b) ester vanillin-benzoate (**1)** (red line), and (c) composite material (**2)** (green line).

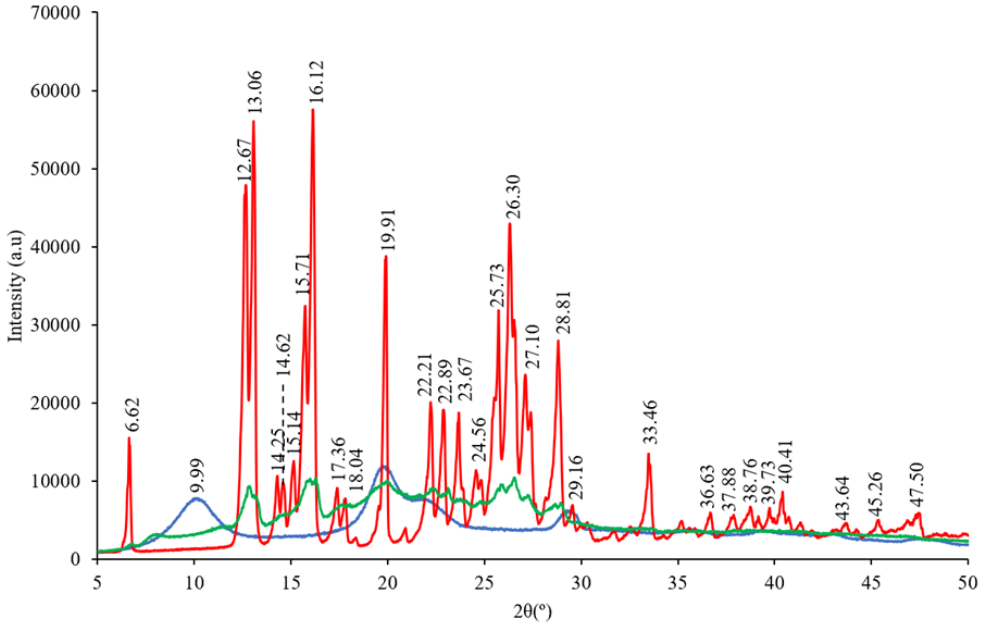

Figure 4. XRD diffractograms of chitosan (blue line), ester vanillin-benzoate (**1)** (red line), and composite material (**2)** (green line).

antimicrobial testing and at 30 °C for antifungal testing. For comparison, chloramphenicol was used as a positive control in antibacterial assays against S. aureus, B. subtilis, E. coli, and P. aeruginosa. Antimicrobial and antifungal tests were performed in duplicate.

2.2.4. Determination of the Degree of Chitosan Deacetylation

The degree of deacetylation (DD) of chitosan was measured using Fourier-transform infrared (FTIR) spectroscopy. Chitosan samples were dried at 50 °C to remove moisture before finely grinding. Spectra were recorded over the 4000–400 cm^{-1} range at 4 cm^{-1} resolution, using 64 scans. After baseline correction, the absorbance intensities at 1320 cm^{-1} (CH_3 deformation of the acetyl group) and 1420 cm^{-1} (CH deformation of the glucosamine ring) were measured, and the ratio A_{1320}/A_{1420} was calculated. The degree of acetylation (DA) was

obtained from a calibration curve developed using known DA standards, and the DD was expressed as DD = 100 – DA [37].

2.2.5. Characterization of Synthesized Compounds

The synthesized composite was characterized using a variety of instrumental techniques. Functional groups were analyzed using FTIR (Bruker Alpha), while the crystal structure was examined through XRD (D6 PHASER). Raman spectroscopy (Bruker Senterra II) revealed the chemical structure and molecular identification, while SEM (Phenom ProX G6) was used to examine the composite's surface shape. The compound 4-formyl-2-methoxyphenyl benzoate (**1**), a vanillin benzoate ester, was characterized using FTIR, ^{1}H-NMR, ^{13}C-NMR, and MS spectroscopic techniques, as presented in Figures 2(a) – (d). Furthermore, the formation of the composite material (**2**) was confirmed through FTIR, XRD,

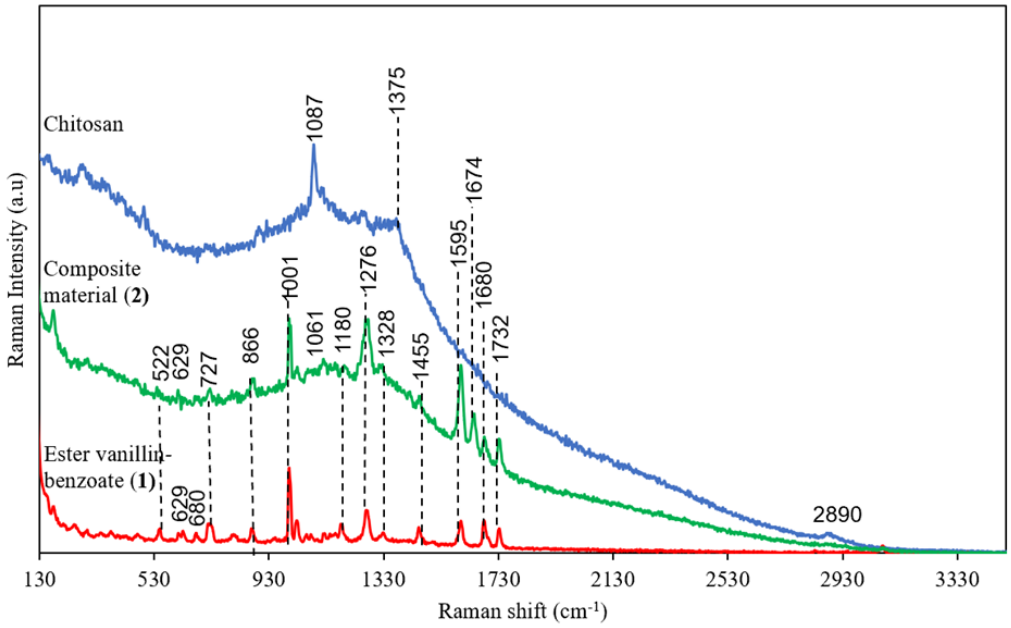

Figure 5. Raman spectra of (a) chitosan (blue line), (b) ester vanillin-benzoate (**1**) (red line), and (c) composite material (**2**) (green line).

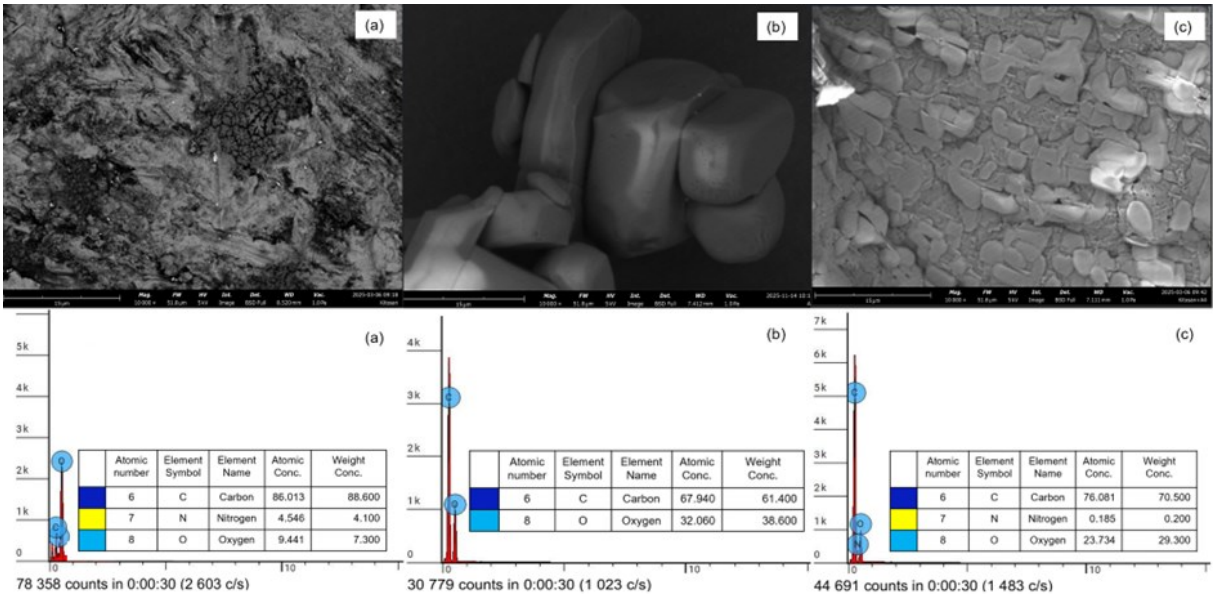

Figure 6. SEM and EDX profiles of (a) chitosan, (b) ester vanillin-benzoate (**1**), and (c) composite material (**2**).

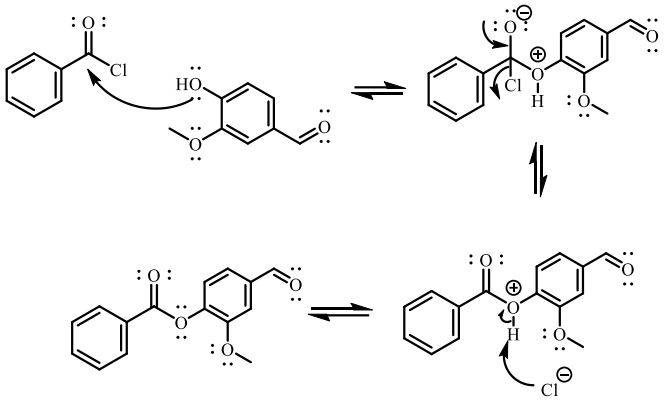

Figure 7. Esterification mechanism of vanillin by benzoyl chloride.

Raman, and SEM analyses (Figures 3 – 6). The synthesis pathway of the composite material is illustrated in Figure 1.

3. RESULTS AND DISCUSSIONS

3.1. 4-formyl-2-methoxyphenyl benzoate (1)

Colourless crystal in 93.28% yield. Melting point (m.p.) 70 °C. FTIR (cm^{-1}), str. = stretching, bend. = bending: 3111 (C–H sp^2 str.), 3004 and 2914 (C–H sp^3 str.), 1732 (C=O str.), 1592 and 1502 (C=C str.), and 1256 (C–O str.). ^{1}H-NMR (ppm): 3.88 (s, 3H, OCH_3), 7.33–7.35 (d, 2H, H_{Ar} vanillin), 7.50–7.52 (t, 2H, H_{Ar} phenyl), 7.53–7.54 (d, 1H, H_{Ar} vanillin), 7.63–7.66 (t, 1H, H_{Ar} phenyl), 8.19–8.22 (d, 2H, H_{Ar} phenyl), 9.97 (s, 1H, CHO). ^{13}C-NMR: 56.22 (OCH_3), 110.96, 123.69, 124.93, 135.57, 145.33; 152.31 (C_{Ar} vanillin), 128.75, 130.50, 133.96 (C_{Ar} phenyl), 164.27 (O–C=O), and 191.25 (CHO). MS (m/z): 256 (M^+), 151, 119, 105 (base peak), 95, 77, 65, 51, 39, and 28. The spectroscopic data are shown in Figure 2.

3.2 Composite Material (2)

Colorless beads in a 90.21% yield and decomposed at 220 °C. FTIR (cm^{-1}): 3062 (C–H sp^2 str.), 3004 and 2914 (C–H sp^3 str.), 1732 (C=O str.), 1592 and 1502 (C=C str.), and 1247 (C–O str.). 2θ (º): 12.29°, 15.98°, 16.26°, 17.89°, 19.97°, 22.29°, 23.11°, 23.71°, 25.91°, 26.55°, 27.29°, 28.94°, and 33.08°. Raman (cm^{-1}): 626 and 727 (C–H out-of-plane substituted benzene ring), 1061 and 1180 (C–O str. and C–H bend.), 1276 and 1328 (C–O–CH_3), 1455 (CH_2/CH_3 in-plane bend.), 1596 (C=C str.), and 1732 (C=O str.).

The synthesis of the composite material in this study involved two consecutive reaction processes. In the first stage, the hydroxyl group of vanillin was esterified with benzoyl chloride, generating colorless crystals of compound **1** (93.28% yield). Figures 2 – 6 provide a complete characterization of the synthesized compound. The FTIR spectra of the compound revealed the absence of vanillin's O –H group, which generally shows at 3400 cm^{-1}. This observation was further confirmed by the ^{1}H-NMR spectra, where the characteristic hydroxyl proton signal of vanillin at 6.39 ppm had disappeared, indicating successful modification of the hydroxyl group during the synthesis process. The aromatic protons corresponding to the benzoate functional group appeared with chemical shifts ranging from 7.50 to 7.66 ppm. Similarly, the ^{13}C -NMR spectra displayed aromatic carbon signals between 128.75 and 133.94 ppm, consistent with the benzoate moieties. Furthermore, the presence of molecular ion peaks in the mass spectrum verified the successful synthesis of the ester vanillin-benzoate (**1**), thereby validating its structural integrity.

Ester vanillin-benzoate (**1**) was reacted with chitosan via a Schiff base reaction in the acidic media, allowing the aldehyde group to react with the chitosan amine group. The resulting composite material (**2**) exhibited satisfactory reactivity and good thermal stability, producing a white solid with a high yield of 90.21% and thermal decomposition at 220 °C. The FTIR spectrum of compound **2** shows absorptions at 1674 cm^{-1} (C=N), 1732 cm^{-1} (C=O), and 1592 and 1502 cm^{-1} (C=C alkene), while chitosan lacks these three absorptions (Figure 3).

The XRD diffractogram of composite material

(**2**) displays 2θ values that correspond to both chitosan and ester vanillin benzoate (**1**), indicating that the ester compound is primarily distributed on the surface of the chitosan matrix. As shown in Figure 4, the XRD pattern reveals characteristic 2θ peaks at 10.08°, 19.91°, and 29.39° for chitosan oligosaccharide; 9.62°, 12.67°, 13.06°, 14.25°, 14.62°, 15.14°, 15.71°, 16.12°, 17.36°, 18.08°, 22.21°, 22.89°, 23.67°, 24.56°, 25.73°, 26.30°, 27.10°, 28.81°, 29.16°, 33.46°, 36.63°, 37.88°, 38.76°, 39.73°, 40.41°, 43.64°, 45.26°, and 47.50° for ester vanillin benzoate (**1**); and 12.29°, 15.98°, 16.26°, 17.89°, 19.97°, 22.29°, 23.11°, 23.71°, 25.91°, 26.55°, 27.29°, 28.94°, and 33.08° for the composite material (**2**).

The XRD spectrum indicates that the ester compound is predominantly distributed on the chitosan matrix's surface, as evidenced by the retention of sharp crystalline peaks and the absence of substantial peak shifts or broadening in the composite pattern. In the XRD analysis, the ester vanillin-benzoate (red line) exhibits multiple sharp and intense peaks, indicating high crystallinity. When incorporated into the chitosan matrix (blue line), these peaks remain mostly unaltered, suggesting that the ester compound retains its crystalline structure and is not disrupted by molecular interactions with chitosan. If the ester were embedded within the chitosan matrix, amorphization or molecular dispersion would cause peak widening or even disappearance. Instead, the composite pattern shows a superposition of the ester's crystalline peaks and the broad amorphous peaks of chitosan (green line), implying surface-level dispersion rather than matrix integration. This is consistent with the findings of Podgorbunskikh et al. [38], who demonstrated that mechanical mixing or surface adsorption of crystalline compounds onto amorphous polymers, such as chitosan, causes the compound to remain structurally intact and externally distributed rather than molecularly dispersed within the chitosan matrix.

The Raman band observed at 1087 cm^{-1} (Figure 5) in chitosan corresponds to C–O–C stretching vibrations due to glycosidic bonds. This feature provides valuable insight into the structural characteristics of the polysaccharide backbone. The Raman peak at 1375 cm^{-1} corresponds to the symmetrical bending of $–CH_3$ groups, suggesting the presence of residual N-acetyl groups and the degree of deacetylation inside the chitosan matrix. The Raman spectrum of composite material (**2**) shows distinctive wavenumbers from both ester vanillin benzoate (**1**) and chitosan, indicating that the ester compound is predominantly distributed on the surface of the chitosan matrix. Raman spectra demonstrate that the vibration observed at 522 cm^{-1} corresponds to skeletal motions in the aromatic

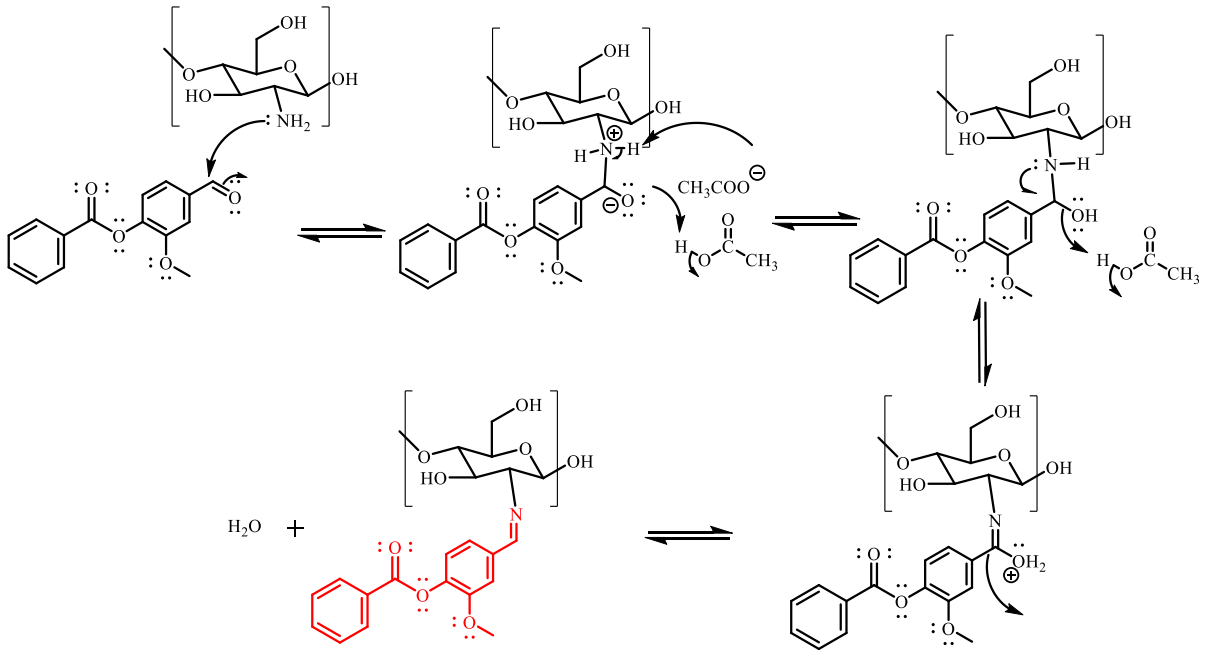

Figure 8. Mechanism for the synthesis of a composite material via the Schiff base reaction.

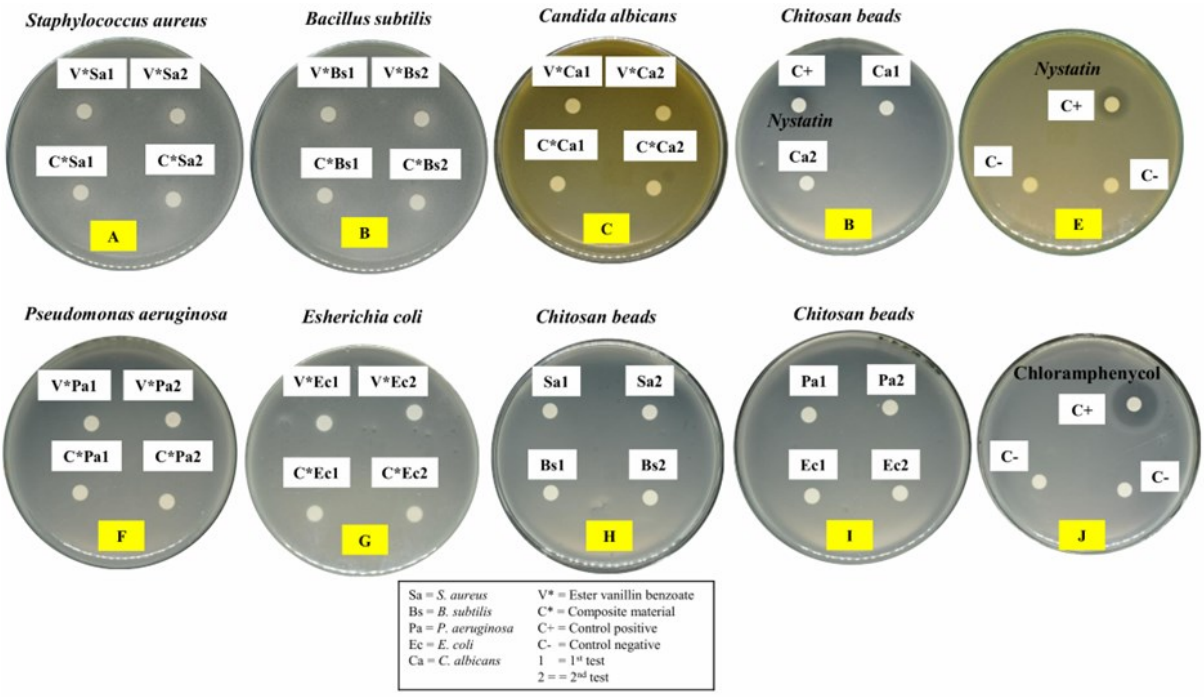

Figure 9. Photographic images of bacterial and fungal inhibition zones of ester vanillin benzoate (**1**), composite material (**2**), and chitosan beads.

ring. Meanwhile, the bands at 626 and 727 cm^{-1} are attributed to C–H out-of-plane bending vibrations in the substituted benzene ring. The prominent signal at 1001 cm^{-1} represents the symmetric ring-breathing mode found in aromatic compounds. The absorption bands at 1061 and 1180 cm^{-1} represent C –O stretching and C–H bending vibrations, respectively. Meanwhile, the signals at 1276 and 1328 cm^{-1} indicate methoxy group vibrations and aromatic ring stretching. The peak at 1455 cm^{-1} denotes CH_2/CH_3 in-plane bending, whereas the band at 1596 cm^{-1} corresponds to C=C stretching inside the aromatic rings. The peak at 1674 cm^{-1} indicates a C=N bond in the composite material (**2**). The stretching vibration of the imine (C=N) functional group is commonly detected at 1650-1690 cm^{-1}. The absorption bands at higher frequencies (1644, 1680, and 1732 cm^{-1}) correspond to conjugated C=O stretching vibrations, confirming esterification and resonance behavior within the vanillin structure.

This study's Raman spectrum results are consistent with those of Xiao Da et al. [39], who discovered that ester and vinyl functionalities retained their characteristic peaks following surface grafting, confirming that Raman spectroscopy effectively distinguishes surface-bound versus embedded molecular interactions. Similarly, Chen et al. [40] demonstrated that chitosan-nanosilver composites used for SERS detection preserved the vibrational modes of adsorbed analytes, supporting the hypothesis that strong Raman signals from the ester compound in their composite arise from surface localization rather than matrix entrapment.

The SEM-EDX analysis provides further confirmation of the successful synthesis. The SEM image of composite material (**2**) (Figure 6(c)) shows a uniform and well-organized surface shape. In contrast, the SEM image of chitosan (Figure 6 (a)) reveals a crumpled, heterogeneous structure characterized by densely packed particles and an irregular, rough surface texture. After modification, SEM analysis of composite material (**2**) revealed a uniform and homogeneous surface morphology. The EDX results for ester vanillin benzoate (**1**) showed the presence of carbon (C) and oxygen (O), whereas both chitosan and the composite material (**2**) contained C, O, and nitrogen (N), as illustrated in Figure 6. The thermal behavior of composite material (**2**) provides additional evidence of its successful synthesis. The composite decomposes at 220 °C, exhibiting higher thermal stability compared to its separate components, chitosan and ester vanillin benzoate (**1**), which have melting

points of 196 and 70 °C, respectively.

The SEM image reveals a heterogeneous surface with identifiable regions. At the same time, the EDX spectrum shows elevated oxygen content and reduced nitrogen content compared to pure chitosan, indicating the presence of predominantly esterified vanillin-benzoate on the surface. This result is consistent with Andrew et al. [41], who reported that chitosan nanocomposites loaded with functional additives exhibited surface roughness and compositional shifts in EDX, confirming surface-level adsorption rather than matrix embedding. These findings are consistent with Lewandowska and Szulc [42], who found that chitosan composites formed via physical mixing retained distinct elemental profiles and surface textures, supporting the non-covalent, superficial distribution of additives.

Vanillin is esterified by benzoyl chloride through a nucleophilic acyl substitution reaction (Figure 7). In this mechanism, vanillin's hydroxyl group serves as a nucleophile, interacting with the electrophilic carbonyl carbon of benzoyl chloride to form an ester bond. This process leads to the formation of a tetrahedral intermediate, which subsequently collapses, releasing a chloride ion and forming an ester bond. The resultant compound, vanillin benzoate, exhibits improved stability and lipophilicity. Gendron [43] describes a similar esterification procedure utilizing vanillin and benzoyl chloride, where vanillin is used as a biosourced building block for various functional derivatives, including esters.

In the subsequent Schiff base reaction, ester vanillin benzoate (**1**) interacts with chitosan to produce a composite material (**2**) through the condensation of imine (C=N) bonds, as illustrated in Figure 8. The aldehyde group of the ester vanillin benzoate forms a strong C=N (Schiff base) bond with the chitosan backbone's primary amine groups. This covalent bond enhances the composite's structural integrity and functional performance, particularly its thermal stability. This is supported by the fact that vanillin benzoate, which melts at 70 °C, has a higher decomposition temperature of approximately 220 °C after being incorporated into the composite, indicating improved thermal stability. In the study by Zhu et al. [44], vanillin-conjugated chitosan emulsions were synthesized via a Schiff base reaction, where the aldehyde group of vanillin reacts with the primary amine group of chitosan while stirring. The mechanism involves a nucleophilic collision by the chitosan amine on the carbonyl carbon of vanillin, forming a tetrahedral intermediate that eliminates water to yield a stable imine (Schiff base) linkage.

3.3. Antibacterial and Antifungal Studies of Vanillin Benzoate Ester (1) and Composite Material (2)

Ester vanillin benzoate (**1**) and its composite material (**2**) were tested for antibacterial and antifungal activity against two Gram-positive bacteria (*S. aureus* and *B. subtilis*), two Gram-negative bacteria (*E. coli* and *P. aeruginosa*), and the fungal strain *C. albicans*. The antibacterial and antifungal properties of the synthesized compounds were compared to those of conventional drugs, chloramphenicol and nystatin. The results, illustrated in Figure 9 and summarized in Table 1, reveal that ester vanillin benzoate (**1**) had moderate antibacterial activity, producing inhibition zones of 10.025 and 10.195 mm against *S. aureus* and *B. subtilis*, respectively. However, after being transformed into a composite material, the inhibition zones increased slightly to 10.665 and 10.215 mm. These findings suggest that both compounds exhibit relatively weak antibacterial activity, which falls within the moderate inhibition zone category according to Davis and Stout [45]. The slight improvement reported in vanillin benzoate ester after insertion into a chitosan-based composite is likely attributable to synergistic interactions between the ester molecule and the biopolymer matrix [46][47]. When vanillin benzoate ester is added to the chitosan matrix, its diffusion and controlled release are increased, thereby allowing longer and more consistent exposure to bacterial cells [48]. Furthermore, the composite structure may improve the ester's solubility and stability, enhancing its bioavailability and capacity to interact with microbial membranes [49]. This synergistic connection between chitosan and the ester molecule contributes to a moderate but significant improvement in antibacterial activity.

Vanillin benzoate ester (**1**) and composite material (**2**) revealed weak antibacterial activity against *S. aureus* and *B. substilis* but showed no

Table 1. Bacterial and fungal inhibition zone by chitosan beads, compounds **1** and **2**, as well as positive controls.

Compounds	Inhibition zone (mm)					
	S. aureus*	***S. aureus*****	***Av. S. aureus***	***B. substilis****	***B. substilis*****	***Av. B. substilis***
Ester vanillin benzoate (**1**)	10.15	9.90	10.025 ± 0.125	9.96	10.43	10.195 ± 0.235
Composite material (**2**)	11.22	10.11	10.665 ± 0.555	10.54	9.89	10.215 ± 0.325
	1	**2**	**Av.**			
Chloramphenicol	18.00	18.01	18.005 ± 0.007			
Nystatin	8.03	8.00	8.015 ± 0.021			
	S. aureus*	***S. aureus*****	***Av. S. aureus***	***B. substilis****	***B. substilis*****	***Av. B. substilis***
Chitosan beads	6.05	6.04	6.045 ± 0.007	6.06	6.08	6.070 ± 0.014
	P. aeruginosa*	***P. aeruginosa*****	***Av. P. aeruginosa***	***E. coli****	***E. coli*****	***E. coli***
	6.02	6.05	6.035 ± 0.021	6.04	6.01	6.025 ± 0.021
	C. albicans*	***C. albicans*****	***C. albicans***			
	6.03	6.07	6.050 ± 0.028			

Note: Ester vanillin benzoate (**1**) and composite material (**2**) did not show antimicrobial and antibacterial activity against *P. aeruginosa, E. coli,* and *C. albicans*, so their activity are not written in Table 1. * = test 1; ** = test 2; Av = average.

antibacterial activity against *E. coli* and *P. aeruginosa*. Furthermore, these compounds exhibited no detectable antifungal activity. This difference mainly arises from the distinct structural organization of bacterial cell walls. Gram-positive bacteria, such as *S. aureus* and *B. subtilis*, possess thick peptidoglycan layers that are more exposed and permeable to external compounds, enabling direct interaction with cell wall or membrane components [50]. In contrast, Gram-negative bacteria, such as *E. coli* and *P. aeruginosa*, have an outer membrane composed of lipopolysaccharides that serve as a selective barrier, preventing the penetration of hydrophobic or large molecules [51]. This structural constraint most likely prevents the active components of compounds (**1**) and (**2**) from penetrating bacterial cells and reaching their intracellular targets, resulting in low antibacterial activity. Consequently, the observed selectivity suggests that their mode of action is more compatible with the physiological structure of Gram -positive bacteria.

Based on Table 1, chitosan beads only form an inhibitor zone of approximately 6 mm against *S. aureus, B. subtilis, P. aeruginosa, E. coli, and C. albicans*. Chitosan beads, due to their larger size and compact matrix, release antimicrobial agents slowly and disperse less effectively in agar-based experiments. This results in smaller inhibition zones despite having the same base material. This is consistent with the findings of Al-Zahrani et al. [52], who discovered that chitosan beads merely provide an inhibition zone of 6–8 mm, much narrower than that of chitosan nanoparticles as antimicrobials and antifungals.

The limited antifungal performance of vanillin benzoate ester (**1**) and its composite material (**2**) against *C. albicans* appears to be linked to their structural characteristics. The phenolic O–H group, which is crucial to antifungal activity, is covered during the esterification of vanillin by benzoic acid, decreasing the compound's capacity to interact effectively with fungal cells. This functional group plays a key role in antifungal activity by disrupting the integrity of fungal cell membranes. When this group is covered by ester formation, the compound loses much of its reactivity, diminishing its ability to inhibit fungal proliferation. Furthermore, when the active substance is incorporated into a composite matrix, it may become physically confined or chemically bound, limiting its release and accessibility to fungal cells. These characteristics work together to prevent fungus from interacting effectively, reducing the antifungal efficacy of both the ester and composite forms.

4. CONCLUSIONS

This study successfully synthesized ester vanillin benzoate (**1**) and its composite material (**2**) derived by a chitosan Schiff base, yielding 93.28% and 90.21%, respectively. The chemical structures of both compounds were fully studied using analytical techniques. The produced compound exhibits weak antibacterial activity against *S. aureus* and *B. subtilis*, with inhibition zones of 10.025 and 10.195 mm, respectively. Interestingly, after being transformed into a composite material, the compound showed increased antibacterial activity, as evidenced by inhibition zone diameters of 10.665 mm and 10.215 mm. In contrast, ester vanillin benzoate (**1**) and a composite material (**2**) are ineffective against *P. aeruginosa*, *E. coli*, and *C. albicans* due to membrane-layer composition discrepancies. Our findings indicate that when vanillin is esterified with benzoic acid, the phenolic hydroxyl group of chitosan, which is responsible for damaging fungal cell membranes, is concealed. Consequently, this modification reduces the compound's ability to interact with the fungal membrane, thereby weakening its antifungal properties. Moreover, when the active compound is added to a composite matrix, its release might be restricted by either physical entrapment within the material or by chemical binding to other components. As a result, its capacity to interact directly with fungal cells diminishes, reducing total antifungal efficacy.

AUTHOR INFORMATION

Corresponding Author

Devi Ratnawati — Department of Chemistry, Universitas Bengkulu (UNIB), Bengkulu-38122 (Indonesia);

orcid.org/0000-0002-4670-8472

Email: deviratnawati@unib.ac.id

Authors

Risky Hadi Wibowo — Department of Biology, Universitas Bengkulu (UNIB), Bengkulu-38122 (Indonesia);
orcid.org/0000-0002-5917-4625

Vicka Andini — Department of Chemistry, Universitas Bengkulu (UNIB), Bengkulu-38122 (Indonesia);
orcid.org/0009-0005-7753-4005

Evi Maryanti — Department of Chemistry, Universitas Bengkulu (UNIB), Bengkulu-38122 (Indonesia);
orcid.org/0000-0002-1392-4662

Yehezkiel Steven Kurniawan — Department of Chemistry, Universitas Gadjah Mada (UGM), Yogyakarta-55281 (Indonesia);
orcid.org/0000-0002-4547-239X

Author Contributions

Conceived and designed the experiments: D. R. Performed the experiments, analysed, and interpreted the data: D. R., Y. S. K., V. A., R. H. W., and E. M. Contributed reagents, materials, analysis tools, or data: D. R. Wrote and revised the manuscript: D. R. and Y. S K. All authors approved the final version of the manuscript.

Conflicts of Interest

The authors have no conflict of interest regarding the publication of this work.

ACKNOWLEDGEMENT

The authors thank to the microbiology laboratory for assisting with the antibacterial and antifungal tests, and to the chemistry laboratory of Universitas Bengkulu for providing FTIR, Raman, XRD, and SEM instruments for structural analysis.

DECLARATION OF GENERATIVE AI

Not applicable.

REFERENCES

[1] S. Naskar, S. Sharma, and K. Kuotsu. (2019). "Chitosan-Based Nanoparticles: An Overview of Biomedical Applications and Its Preparation". *Journal of Drug Delivery Science and Technology.* **49** : 66-81. 10.1016/j.jddst.2018.10.022.

[2] M. Ul-Islam, K. F. Alabbosh, S. Manan, S. Khan, F. Ahmad, and M. W. Ullah. (2024). "Chitosan-Based Nanostructured Biomaterials: Synthesis, Properties, and Biomedical Applications". *Advanced Industrial and Engineering Polymer Research.* **7** (1): 79-99. 10.1016/j.aiepr.2023.07.002.

[3] R. Román-Doval, S. P. Torres-Arellanes, A. Y. Tenorio-Barajas, A. Gómez-Sánchez, and A. A. Valencia-Lazcano. (2023). "Chitosan: Properties and Its Application in Agriculture in the Context of Molecular Weight". *Polymers.* **15** (13): 2867. 10.3390/polym15132867.

[4] S. Khattak, F. Wahid, L. P. Liu, S. R. Jia, L. Q. Chu, Y. Y. Xie, A. X. Li, and C. Zhong. (2019). "Applications of Cellulose and Chitin/Chitosan Derivatives and Composites as Antibacterial Materials: Current State and Perspectives". *Applied Microbiology and Biotechnology.* **103** (5): 1989-2006. 10.1007/s00253-018-09602-0.

[5] H. P. S. A. Khalil, C. K. Saurabh, M. N. Fazita, M. I. Syakir, Y. Davoudpour, M. Rafatullah, C. K. Abdullah, M. K. M. Haafiz, and R. Dungani. (2016). "A Review on Chitosan–Cellulose Blends and Nanocellulose-Reinforced Chitosan Biocomposites: Properties and Their Applications". *Carbohydrate Polymers.* **150** : 216-226. 10.1016/j.carbpol.2016.05.028.

[6] J. D. Giraldo and B. L. Rivas. (2021). "Direct Ionization and Solubility of Chitosan in Aqueous Solutions by Acetic Acid". *Polymer Bulletin.* **78** (3): 1465-1488. 10.1007/s00289-020-03172-w.

[7] S. Mohebbi, M. N. Nezhad, P. Zarrintaj, S. H. Jafari, S. S. Gholizadeh, M. R. Saeb, and M. Mozafari. (2019). "Chitosan in Biomedical Engineering: A Critical Review". *Current Stem Cell Research & Therapy.* **14** (2): 93-116. 10.2174/1574888X13666180912142028.

[8] R. Lima, C. Fernandes, and M. M. Pinto. (2022). "Molecular Modifications, Biological Activities, and Applications of Chitosan and

Derivatives: A Recent Update". *Chirality.* **34** (9): 1166-1190. 10.1002/chir.23477.

[9] J. Tarique, S. M. Sapuan, N. F. Aqil, A. Farhan, J. I. Faiz, and S. Shahrizan. (2023). In: "Composites from the Aquatic Environment". 3855-3891. 10.1007/978-981-19-5327-9_1.

[10] A. O. Francis, M. A. A. Zaini, I. M. Muhammad, S. Abdulsalam, and U. A. El-Nafaty. (2023). "Physicochemical Modification of Chitosan Adsorbent: A Perspective". *Biomass Conversion and Biorefinery.* **13** (7): 5557-5575. 10.1007/s13399-021-01599-3.

[11] K. F. Mohammed and H. A. Hasan. (2022). "Synthesis, Chemical and Biological Activity Studies of Azo–Schiff Base Ligand and Its Metal Complexes". *Chemical Methodologies.* **6** (12): 905-913. 10.22034/CHEMM.2022.353591.1584.

[12] X. Zhao, S. Feng, S. Li, Y. Hu, W. Wang, X. Zhang, Q. Zhang, Y. Chen, J. Liu, and L. Ma. (2023). "The Role of Primary Amines in Modified Chitosan to Enhance the Aldol Condensation of Biomass-Derived Carbonyl Compounds". *Fuel.* **351** : 128820. 10.1016/j.fuel.2023.128820.

[13] A. Moanta. (2025). "Classification, Synthesis, Isomerism, and Spectral Characterization of Schiff Bases". *Mini-Reviews in Organic Chemistry.* **22** (7): 718-737. 10.2174/0118756298326751241031103603.

[14] A. Jain, S. De, and P. Barman. (2022). "Microwave-Assisted Synthesis and Notable Applications of Schiff Base and Metal Complexes: A Comparative Study". *Research on Chemical Intermediates.* **48** (5): 2199-2251. 10.1007/s11164-022-04708-7.

[15] A. G. Taha, M. F. Radwan, M. E. Abdu, N. M. Ali, and M. R. Eletmany. (2024). "Green Synthesis and Applications of Modified Schiff Base Chitosan Derivatives". *African Journal of Biomedical Research.* **27** (4S): 58-64. 10.53555/AJBR.v27i4S.3498.

[16] N. Çelikçi, C. A. Zıba, and M. Tümer. (2025). "Chitosan-Based Schiff Base Compounds: Synthesis, Chemical Characterization, and Antibacterial Properties". *Journal of Fluorescence.* 1-11. 10.1007/s10895-025-04233-x.

[17] M. Al-Mosawy. (2023). "Review of the Biological Effects of Schiff Bases and Their Derivatives, Including Their Synthesis". *Medical Science Journal for Advanced Research.* **4** (2): 67-85. 10.46966/msjar.v4i2.117.

[18] T. M. Tamer, M. A. Hassan, A. M. Omer, W. M. Baset, M. E. Hassan, M. E. El-Shafeey, and M. S. M. Eldin. (2016). "Synthesis, Characterization, and Antimicrobial Evaluation of Two Aromatic Chitosan Schiff Base Derivatives". *Process Biochemistry.* **51** (10): 1721-1730. 10.1016/j.procbio.2016.08.002.

[19] G. K. Moore and G. A. Roberts. (1981). "Reactions of Chitosan: III. Preparation and Reactivity of Schiff Base Derivatives of Chitosan". *International Journal of Biological Macromolecules.* **3** (5): 337-340. 10.1016/0141-8130(81)90053-2.

[20] A. A. Alamri, R. M. Borik, A. H. A. El-Wahab, H. M. Mohamed, K. S. Ismail, M. R. El-Aassar, A. A. M. Al-Dies, and A. M. El-Agrody. (2025). "Synthesis of Schiff Bases Based on Chitosan: Thermal Stability and Evaluation of Antimicrobial and Antitumor Activities". *Scientific Reports.* **15** (1): 892. 10.1038/s41598-024-73610-6.

[21] I. Mushtaq, M. Ahmad, M. Saleem, and A. Ahmed. (2024). "Pharmaceutical Significance of Schiff Bases: An Overview". *Future Journal of Pharmaceutical Sciences.* **10** (1): 16. 10.1186/s43094-024-00594-5.

[22] M. Ismaeel, B. Parveen, S. S. Dogar, K. Aftab, K. Abbas, and K. S. Munawar. (2024). "Comparing Green and Conventional Methods for Schiff Base Synthesis and Unveiling Environmental Stability Applications: A Review". *Journal of Coordination Chemistry.* **77** (9-10): 921-959. 10.1080/00958972.2024.2362344.

[23] J. Chen, F. Xie, X. Li, and L. Chen. (2018). "Ionic Liquids for the Preparation of Biopolymer Materials for Drug and Gene Delivery: A Review". *Green Chemistry.* **20** (18): 4169-4200. 10.1039/C8GC01120F.

[24] P. Berton and J. L. Shamshina. (2023). "Ionic Liquids as Tools to Incorporate Pharmaceutical Ingredients into Biopolymer-Based Drug Delivery Systems". *Pharmaceuticals.* **16** (2): 272. 10.3390/ph16020272.

[25] N. Q. Haj, M. O. Mohammed, and L. E. Mohammood. (2020). "Synthesis and Biological Evaluation of Three New Chitosan Schiff Base Derivatives". *ACS Omega.* **5** (23): 13948-13954. 10.1021/acsomega.0c01342.

[26] A. M. Y. Moustafa, M. M. Fawzy, M. S. Kelany, Y. A. Hassan, R. F. Elsharaawy, and F. H. Mustafa. (2024). "Synthesis of New Quaternized Chitosan Schiff Bases and Their N-Alkyl Derivatives as Antimicrobial and Anti-Biofilm Retardants in Membrane Technology". *International Journal of Biological Macromolecules.* **267** : 131635. 10.1016/j.ijbiomac.2024.131635.

[27] S. Kim. (2018). "Competitive Biological Activities of Chitosan and Its Derivatives: Antimicrobial, Antioxidant, Anticancer, and Anti-Inflammatory Activities". *International Journal of Polymer Science.* 1708172. 10.1155/2018/1708172.

[28] S. S. Ali, E. R. Kenawy, F. I. Sonbol, J. Sun, M. Al-Etewy, A. Ali, L. Huizi, and N. A. El-Zawawy. (2019). "Pharmaceutical Potential of a Novel Chitosan Derivative Schiff Base with Special Reference to Antibacterial, Anti -Biofilm, Antioxidant, Anti-Inflammatory, Hemocompatibility, and Cytotoxic Activities". *Pharmaceutical Research.* **36** (1): 5. 10.1007/s11095-018-2535-x.

[29] M. A. Ali, K. A. Aswathy, G. Munuswamy-Ramanujam, and V. Jaisankar. (2023). "Pyridine- and Isoxazole-Substituted 3-Formylindole-Based Chitosan Schiff Base Polymer: Antimicrobial, Antioxidant, and In Vitro Cytotoxicity Studies on THP-1 Cells". *International Journal of Biological Macromolecules.* **225** : 1575-1587. 10.1016/j.ijbiomac.2022.11.214.

[30] T. H. Abdalla, A. G. Ibrahim, S. Elabbady, E. Nassar, A. A. Hamed, and A. Aboelnaga. (2025). "Chitosan-Based Schiff Base Polymer Derived from Acetyl Triazolyl Uracil: Synthesis, Characterization, Evaluation of Antimicrobial and Antioxidant Activities, and Density Functional Theory Calculations". *International Journal of Biological Macromolecules.* **300** : 140327. 10.1016/j.ijbiomac.2025.140327.

[31] M. A. Hassan, T. M. Tamer, A. M. Omer, W. M. Baset, E. Abbas, and M. S. Mohy-Eldin. (2023). "Therapeutic Potential of Two Formulated Novel Chitosan Derivatives with Prominent Antimicrobial Activities against Virulent Microorganisms and Safe Profiles toward Fibroblast Cells". *International Journal of Pharmaceutics.* **634** : 122649. 10.1016/j.ijpharm.2023.122649.

[32] A. A. Hamed, G. R. Saad, I. A. Abdelhamid, M. M. Abdel-Aziz, H. A. Taha, M. M. Abou El Dahab, and M. Z. Elsabee. (2022). "Chitosan Schiff Bases/Silver Nanoparticles: Synthesis, Characterization, Antibiofilm and Preliminary Anti-Schistosomal Activity Studies". *Polymer Bulletin.* **79** (12): 11259-11284. 10.1007/s00289-021-03993-3.

[33] A. A. Hamed, I. A. Abdelhamid, G. R. Saad, N. A. Elkady, and M. Z. Elsabee. (2020). "Synthesis, Characterization and Antimicrobial Activity of Novel Chitosan Schiff Bases Based on Heterocyclic Moieties". *International Journal of Biological Macromolecules.* **153** : 492-501. 10.1016/j.ijbiomac.2020.02.302.

[34] B. Nandini and M. A. Selvi. (2025). "Metal Complexes of Schiff Bases: A Review of Their Antimicrobial Activities". *Current Bioactive Compounds.* **21** (5): E15734072305971. 10.2174/0115734072305971240816114116.

[35] J. Ceramella, D. Iacopetta, A. Catalano, F. Cirillo, R. Lappano, and M. S. Sinicropi. (2022). "A Review on the Antimicrobial Activity of Schiff Bases: Data Collection and Recent Studies". *Antibiotics.* **11** (2): 191. 10.3390/antibiotics11020191.

[36] S. T. Rabie, R. A. Abdel-Monem, O. M. Darwesh, and S. T. Gaballah. (2023). "Synthesis and Characterization of Functionalized Modified PVC–Chitosan as Antimicrobial Polymeric Biomaterial".

Polymer Bulletin. **80** (8): 8899-8918. 10.1007/s00289-022-04478-7.

[37] D. I. Sánchez-Machado, J. López-Cervantes, A. A. Escárcega-Galaz, O. N. Campas-Baypoli, D. M. Martínez-Ibarra, and S. Rascón-León. (2024). "Measurement of the Degree of Deacetylation in Chitosan Films by FTIR, 1H NMR, and UV Spectrophotometry". *MethodsX.* **12** : 102583. 10.1016/j.mex.2024.102583.

[38] E. Podgorbunskikh, T. Kuskov, D. Rychkov, O. Lomovskii, and A. Bychkov. (2022). "Mechanical Amorphization of Chitosan with Different Molecular Weights". *Polymers.* **14** (20): 4438. 10.3390/polym14204438.

[39] X. D. Ren, Q. S. Liu, H. Feng, and X. Y. Yin. (2014). "Characterization of Chitosan Nanoparticles by Raman Spectroscopy". *Applied Mechanics and Materials.* **665** 367-370. 10.4028/www.scientific.net/AMM.665.367.

[40] Y. T. Chen and S. C. Shi. (2025). "Development of a Chitosan–Nanosilver Composite as a Surface-Enhanced Raman Scattering-Based Sensor for Bisphenol A Detection". *Sensors and Materials.* **37** (5): 1835-1851. 10.18494/SAM5447.

[41] E. C. Andrew, E. A. Grace, O. E. Chinemerem, and O. E. Emeka. (2025). "Mini Review on Morphological and Microanalysis Characterization of Chitosan Nanocomposites Using Scanning Electron Microscopy". *Mathews Journal of Pharmaceutical Science.* **9** (3): 1-6. 10.30654/MJPS.10052.

[42] K. Lewandowska and M. Szulc. (2022). "Rheological and Film-Forming Properties of Chitosan Composites". *International Journal of Molecular Sciences.* **23** (15): 8763. 10.3390/ijms23158763.

[43] D. Gendron. (2022). "Vanillin: A Promising Biosourced Building Block for the Preparation of Various Heterocycles". *Frontiers in Chemistry.* **10** : 949355. 10.3389/fchem.2022.949355.

[44] J. Zhu, T. Huang, X. Chen, D. Tian, L. Wang, and R. Gao. (2023). "Preparation and Characterization of Vanillin-Conjugated Chitosan-Stabilized Emulsions via a Schiff-Base Reaction". *Food Science and Biotechnology.* **32** (11): 1489-1499. 10.1007/s10068-023-01277-2.

[45] W. W. Davis and T. T. Stout. (1971). "Disc Plate Method of Microbiological Antibiotic Assay: I. Factors Influencing Variability and Error". *Applied Microbiology.* **22** (4): 659-665. 10.1128/am.22.4.659-665.1971.

[46] M. Stroescu, A. Stoica-Guzun, G. Isopencu, S. I. Jinga, O. Parvulescu, T. Dobre, and M. Vasilescu. (2015). "Chitosan–Vanillin Composites with Antimicrobial Properties". *Food Hydrocolloids.* **48** : 62-71. 10.1016/j.foodhyd.2015.02.008.

[47] M. Bustamante-Torres, B. Arcentales-Vera, J. Estrella-Nuñez, H. Yánez-Vega, and E. Bucio. (2022). "Antimicrobial Activity of Composites Based on Biopolymers". *Macromol.* **2** (3): 258-283. 10.3390/macromol2030018.

[48] S. Kamaraj, U. M. Palanisamy, M. S. B. K. Mohamed, A. Gangasalam, G. A. Maria, and R. Kandasamy. (2018). "Curcumin Drug Delivery by Vanillin–Chitosan-Coated Calcium Ferrite Hybrid Nanoparticles as a Carrier". *European Journal of Pharmaceutical Sciences.* **116** : 48-60. 10.1016/j.ejps.2018.01.023.

[49] S. Feng, L. Wang, P. Shao, P. Sun, and C. S. Yang. (2022). "A Review on Chemical and Physical Modifications of Phytosterols and Their Influence on Bioavailability and Safety". *Critical Reviews in Food Science and Nutrition.* **62** (20): 5638-5657. 10.1080/10408398.2021.1888692.

[50] M. Rohde. (2019). In: "Gram-Positive Pathogens, Third Edition". 10.1128/9781683670131.ch1.

[51] H. I. Zgurskaya and V. V. Rybenkov. (2020). "Permeability Barriers of Gram-Negative Pathogens". *Annals of the New York Academy of Sciences.* **1459** (1): 5-18. 10.1111/nyas.14134.

[52] S. S. Al-Zahrani, R. S. Bora, and S. M. Al-Garni. (2021). "Antimicrobial Activity of Chitosan Nanoparticles". *Biotechnology and Biotechnological Equipment.* **35** (1): 1874-1880. 10.1080/13102818.2022.2027816.